Flow Analysis and Design of Three-Dimensional Wind Tunnel Contractions

Yao-xi Su*
Northwestern Polytechnical University, Xian 710072, People's Republic of China

Remarkable progress has been made in the investigation of wind tunnel contractions since the introduction of numerical analysis. However, until recently, most of the work is concerned with two-dimensional or axisymmetric contractions. In the present paper a numerical analysis of incompressible potential flow in wind tunnel contractions with rectangular cross section is conducted. Criteria for the design and performance comparisons of such contractions are discussed, with emphasis on the representation of three-dimensional effects. Five criteria are suggested, including pressure extrema, flow nonuniformity, and crossflow features, which are thought to be useful in the design of rectangular contractions. Contours of a single-parameter family are employed to facilitate the study. Seven geometric parameters are required to define a rectangular contraction. The main subject of this work is a comparative parametric study in which a systematic investigation of the relation between the geometric parameters and the design criteria of three-dimensional contractions is attempted.

Nomenclature

A	= area of cross section
AR	= aspect ratio of cross sections
B	= width of contractions
b	= half-width
CF	= crossflow criterion
CR	= contraction ratio
Cp	= pressure coefficient
D	= square root of cross section area A
H	= height of contractions
h	= half-height
L	= length of contractions
Lt	= total length of extended contractions
n	= power factor of the polynomials
u	= axial velocity
u_w, u_r, u_c	= velocity on the wall, roof, and at the corner
$\bar{u}$	= criterion for flow nonuniformity
X	= match point location of the contours
x, y, z	= Cartesian coordinates
ξ, η, ζ	= transformed coordinates
ϕ	= velocity potential

Subscripts

r	= roof
w	= wall
1	= entrance
2	= exit

I. Introduction

THE contraction nozzle is one of the most important components of a wind tunnel which serves to improve flow uniformity and steadiness and to reduce the turbulence level in the test section. The flow analysis and design of wind tunnel contractions have been the subject of many investigations. However, until recently, most of the work is mainly concerned with the analytical solution of inviscid flow in the contractions. Two-dimensional solutions were obtained by conformal transformation[1] or hodograph methods.[2,3] Solutions of flow in axisymmetric contractions are usually based on power series solution of the Laplace equation or the Stokes-Beltrami equation.[4-10] Although elegant, the analytical solutions are difficult to use because of the mathematics involved. With little regard for design criteria and real conditions in wind tunnel contractions, these solutions are tools of flow analysis, rather than methods of contraction design. In many of the analytical investigations, especially for axisymmetric contractions, an infinite contraction length is assumed. The fact that all contractions are of finite length has important consequences. For finite length contractions velocity extrema and adverse pressure gradients exist near the ends, giving rise to the possibility of boundary-layer separation, a most important problem to be dealt with in contraction design. In connection with these local velocity extrema in finite length contractions, the exit velocity profile can never be uniform, another important problem to be considered in the design.

The problem of designing true finite length contractions with practical criteria was investigated by Morel[11] and others.[12-15] Remarkable progress has been made. However, nearly all of this research is concerned with two-dimensional or axisymmetric contractions. In reality, most wind tunnel contractions are three-dimensional; many of them are of rectangular cross section. Three-dimensionality will cause new phenomena in contraction flow, such as crossflow and the aggravation of velocity extrema at the corner. Only a few works are known to deal with the analysis of three-dimensional contractions.[16-18] Each of these works employed a numerical approach based on finite difference forms of the equations of motion. They differed, however, in grid formation and method of solution. References 17 and 18 also included a study of three-dimensional contraction design. The effects of some geometric parameters on contraction design were investigated. In the present paper, a numerical analysis of incompressible potential flow in contractions with rectangular cross section is conducted. Special attention is directed to a discussion of design criteria and geometric parameters appropriate for three-dimensional contractions.

II. Numerical Analysis

The flow in a contraction bounded by constant-area sections upstream and downstream is analyzed, which is called an "extended contraction." Body-fitted coordinates are used that transform the flowfield of the extended contraction into a unit cube in computational space. The flow equation is transformed accordingly and discretized using an approximate fac-

Received July 30, 1990; revision received April 27, 1991; accepted for publication April 29, 1991.

*Associate Professor, Department of Aircraft Engineering, Member AIAA.

torization scheme AF1. The difference equation is then solved by the ADI technique. A brief description of the technique is given in this section.

Assume that flow in the contraction is incompressible and irrotational, with a velocity potential ϕ which satisfies Laplace's equation

$$\phi_{xx} + \phi_{yy} + \phi_{zz} = 0 \tag{1}$$

Denoting the total length of the extended contraction Lt, width $B(x) = 2b(x)$, height $H(x) = 2h(x)$, the boundary conditions are

$$\phi_y = \pm b'(x)\phi_x \qquad \text{at } y = \pm b(x) \tag{2a}$$

$$\phi_z = \pm h'(x)\phi_x \qquad \text{at } z = \pm h(x) \tag{2b}$$

The conditions at the corner are

$$\phi_y = \pm b'(x)\phi_x, \quad \phi_z = \pm h'(x)\phi_x$$

$$\text{at } y = \pm b(x), \quad z = \pm h(x) \tag{2c}$$

The inclusion of constant-area sections upstream and downstream is necessary in the analysis because of the elliptic nature of Eq. (1). It is assumed that both ends of the extended contraction are sufficiently far to justify the inlet and outlet conditions:

$$\phi(0, y, z) = 0 \tag{3a}$$

$$\phi(Lt, y, z) = K \tag{3b}$$

implying that crossflow velocity components are equal to zero there. Here K is a constant controlling the total flux which can be set equal to one without loss of generality. Numerical tests were made for choosing the minimum length of parallel sections. Denoting the contraction length by L, then $0.5\,L$ is chosen for the upstream section and $0.2\,L$ for the downstream. The errors of velocity calculations are within 1% compared to the results of longer sections. Because of symmetry, only the regions of $y \geq 0$ and $z \geq 0$ need to be calculated, and the condition on the planes of symmetry is that the normal velocities there are equal to zero.

Introducing body-fitted coordinates (ξ, η, ζ) with the definition

$$x = Lt\xi, \qquad y = b(x)\eta, \qquad z = h(x)\zeta \tag{4}$$

the flowfield of the extended contraction is then transformed into a unit cube

$$0 \leq \xi \leq 1, \qquad 0 \leq \eta \leq 1, \qquad 0 \leq \zeta \leq 1 \tag{5}$$

and the flow equation becomes

$$A_{11}\phi_{\xi\xi} + A_{22}\phi_{\eta\eta} + A_{33}\phi_{\zeta\zeta} + A_{12}\phi_{\xi\eta} + A_{13}\phi_{\xi\zeta} + A_{23}\phi_{\eta\zeta} + A_2\phi_\eta + A_3\phi_\zeta = 0 \tag{6}$$

The coefficients A_{11}, and so forth can be obtained easily from the geometric relations (4).

Denoting $\Delta\xi$, $\Delta\eta$, $\Delta\zeta$ as steps in three space directions, and Δt as a step of iteration time, and defining

$$\phi^n_{ijk} = \phi((i-1)\Delta\xi, (j-1)\Delta\eta, (k-1)\Delta\zeta, n\Delta t) \tag{7}$$

the difference equation has the form

$$\left(\alpha - A_{11}\frac{\delta_{\xi\xi}}{\Delta\xi^2}\right)\left(\alpha - A_{22}\frac{\delta_{\eta\eta}}{\Delta\eta^2}\right)\left(\alpha - A_{33}\frac{\delta_{\zeta\zeta}}{\Delta\zeta^2}\right)\Delta^n_{ijk} = 2\alpha^2 L\phi^n_{ijk} \tag{8}$$

where $\Delta^n_{ijk} = \phi^{n+1}_{ijk} - \phi^n_{ijk}$, α is a constant controlling the convergence, $\delta_{\xi\xi}$, $\delta_{\eta\eta}$, $\delta_{\zeta\zeta}$ are operators of second-order centered differences, and L is the difference operator of Eq. (6). In the computations ϕ^{n+1}_{ijk} are calculated from ϕ^n_{ijk} using Eqs. (8) and (3); then the values of ϕ on the lateral boundary are corrected making use of boundary conditions (2).

A grid of 51 × 10 × 10 points is used. The results are found insensitive to a further increase of grid points. No numerical instability has been experienced in the computations. For the present study, high accuracy is not emphasized; typically convergence is accepted with a residual error of $|\Delta^n_{ijk}|_{\max}$ of about 10^{-4}.

III. Criteria of Rectangular Contraction Design

Morel has suggested three criteria for the design of axisymmetric contractions, namely Cp_1, Cp_2, and $\bar{u}_2$, defined as

$$Cp_1 = 1 - \left(\frac{u_{\min}}{u_1}\right)^2 \tag{9a}$$

$$Cp_2 = 1 - \left(\frac{u_2}{u_{\max}}\right)^2 \tag{9b}$$

$$\bar{u}_2 = \frac{u_{2\max} - u_{2\min}}{u_2} \tag{9c}$$

For contractions with contours of a one-parameter, matched-cubic family, he found that the adverse pressure gradients are a function of the Cps only and that the exit nonuniformity $\bar{u}_2$ is related uniquely to Cp_2. Hence, only two criteria are needed, i.e., Cp_1 and $\bar{u}_2$.

For three-dimensional contractions the problem of criteria is more complicated. First, there is no simple criterion (such as Stratford's) for three-dimensional boundary-layer separation prediction. Second, crossflow is a new factor that may cause undesirable boundary-layer thickening or separation, and it is not very clear how to describe this effect quantitatively. Finally, there is one more geometric dimension that will cause complications. Because of these, some empiricism is unavoidable in the design of three-dimensional contractions at the present time. To some extent one still has to rely on the methods and experiences of axisymmetric contraction design. Here a number of criteria are suggested that are thought to be useful in the design of rectangular contractions, particularly from a comparative point of view.

1) *Undershoot near entrance of Cp_1*—For rectangular contractions three Cp (instead of only one) can be defined, i.e., those on the roof, wall, and corner. However, the undershoot at the corner is always a maximum. In the discussion below only Cp_1 defined at the corner is considered, but in some cases Cp_1 on the roof and wall may also be discussed.

2) *Overshoot near exit of Cp_2*—It is found from the computation that in most cases velocity overshoot on the roof and the wall are negligible or simply nonexistent. Hence, Cp_2 is always defined at the corner.

3) *Nonuniformity at exit of $\bar{u}_2$*—For rectangular nozzles the maximum velocity at the exit cross section is always at the corner and the minimum at the center. $\bar{u}_2$ is always larger than its counterpart for axisymmetric nozzles.

4) *Nonuniformity at entrance of $\bar{u}_1$*—This is a measure of upstream influence of the contraction, which may be of importance in some cases, e.g., for the design of turbulence managing devices in a settling chamber or for wind tunnels with tandem test sections. It is thus included as a criterion.

5) *Crossflow criterion CF*—Crossflow criteria on the wall and roof are defined as

$$CF_w = \frac{|u_c^2 - u_w^2|}{u_w^2} \qquad \text{and} \qquad CF_r = \frac{|u_c^2 - u_r^2|}{u_r^2} \tag{10}$$

where u_w, u_r, and u_c are velocities on the wall, roof, and at the corner in one and the same section, and CF_w and CF_r are the maximum values of all sections. Of these two values the larger one is defined as the overall crossflow criterion CF of the contraction. It is thought that CF is a measure of crossflow strength in the boundary layer, with the numerator representing the lateral pressure difference, and the denominator proportional to the kinetic energy of the local boundary-layer flow.

IV. Comparative Parameter Study

For axisymmetric contractions of a one-parameter family contour, three parameters are sufficient to define the geometry, i.e., the area ratio CR, the relative length L/D_1, and the contour parameter, e.g., the match point location X for a cubic family contour.[11] In the present study the concept of one-parameter family contours is also adopted. The investigation is restricted to the contours of matched curves of the form:

$$F = \begin{cases} 1 - \dfrac{(x/L)^n}{X^{n-1}} & 0 \le x/L \le X \\ 1 - \dfrac{(1 - x/L)^n}{(1 - X)^{n-1}} & X \le x/L \le 1 \end{cases} \tag{11}$$

where F stands for $(H - H_2)/(H_1 - H_2)$ or $(B - B_2)/(B_1 - B_2)$. For such contractions there appear to be seven parameters, namely CR; L/D_1; aspect ratios at the entrance and exit, $AR1$ and $AR2$; contour match point of the wall and the roof; Xw and Xr; and the power factor n. The influence of these parameters on the flow and on the design criteria of the contraction are examined below. When one parameter is varied, the rest will take default values if not otherwise stated, namely $CR = 9$; $L/D_1 = 0.833$; $AR1 = AR2 = 1$; $Xw = Xr = 0.5$; and $n = 3$.

A. Length L/D_1

The effect of L/D_1 is shown in Figs. 1 and 2. The range of variation is from 0.4 to 2.0. As L/D_1 increases, pressure gradients, uniformity, and crossflow features are all improved, as expected from the results of axisymmetric studies. However, the values of Cp_1, Cp_2, $\bar{u}_1$, and $\bar{u}_2$ are higher now compared to their counterparts for axisymmetric nozzles due to the corner effect. If the same Cp values are required for rectangular and axisymmetric contractions, the computations show that an increase of the length by 20–25% is needed for rectangular configurations. Figure 2 shows how the contraction length affects the corner velocity distributions and their extrema, illustrating the physical background of the results in Fig. 1. Logarithmic scale is employed for corner velocity u_c. Vertical variation in the plot is $d(\log u_c)$, i.e., du_c/u_c, which weighs the effect of velocity variation more appropriately, particularly for the undershoots.

B. Shape Parameter X (for $Xw = Xr$)

Here Xw and Xr are assumed equal and denoted with a single notation X. Figures 3 and 4 show the effect of its variation, ranging from 0.2 to 0.8. An increase of X will improve (i.e., reduce) the criteria of the entrance, Cp_1 and $\bar{u}_1$, and degrade (i.e., increase) the criteria of the exit, Cp_2 and $\bar{u}_2$. However, it has only a minor effect on the crossflow condition CF. In contraction design, X is a parameter to be optimized for the best compromise of entrance and exit conditions as it is for axisymmetric nozzles.

C. Contraction Ratio CR

In the present study the value of CR was varied from 3 to 30. A decrease of CR has an effect similar to an increase of X, namely improving the entrance condition and worsening the exit condition (see Figs. 5 and 6). If X is properly adjusted

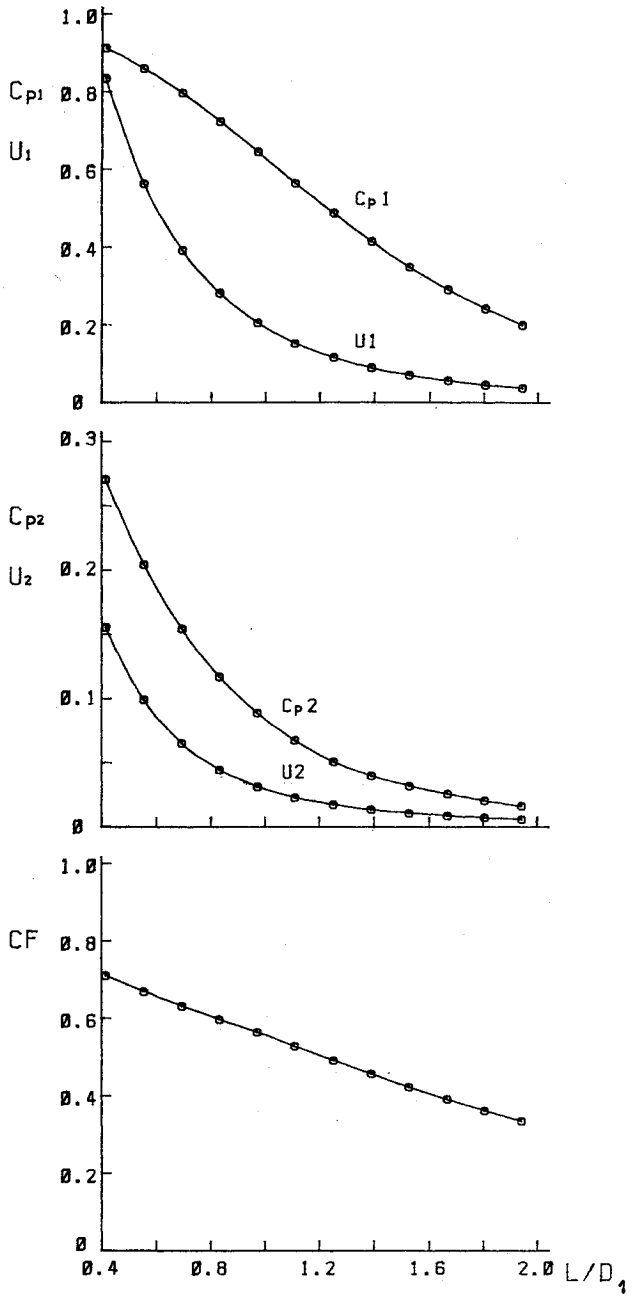

Fig. 1 Effect of length L/D_1 on the design criteria.

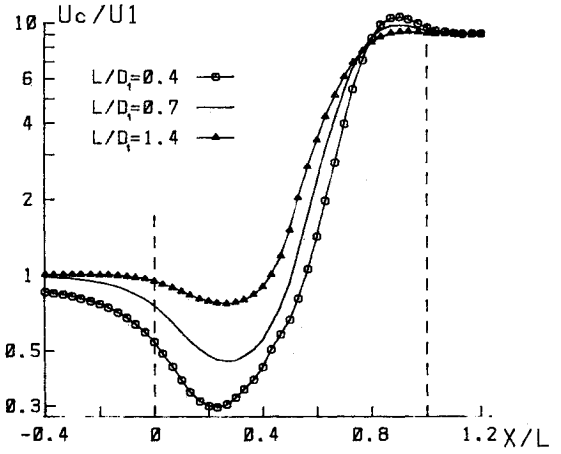

Fig. 2 Effect of L/D_1 on velocity distributions at the corner.

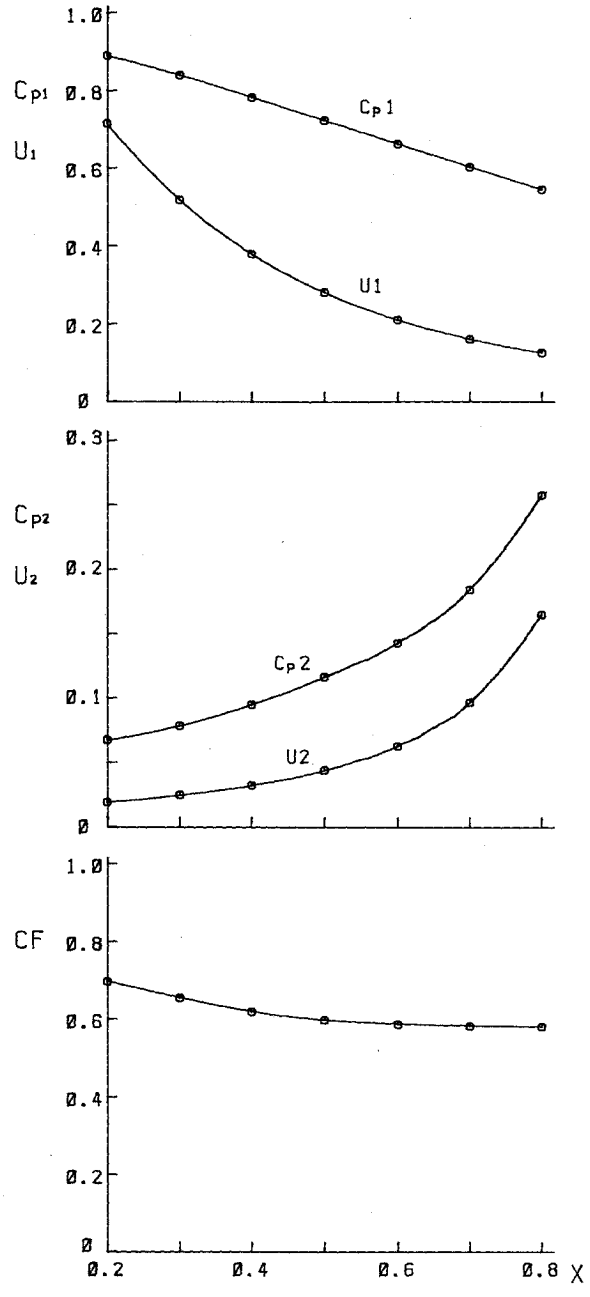

Fig. 3 Effect of parameter X on the design criteria.

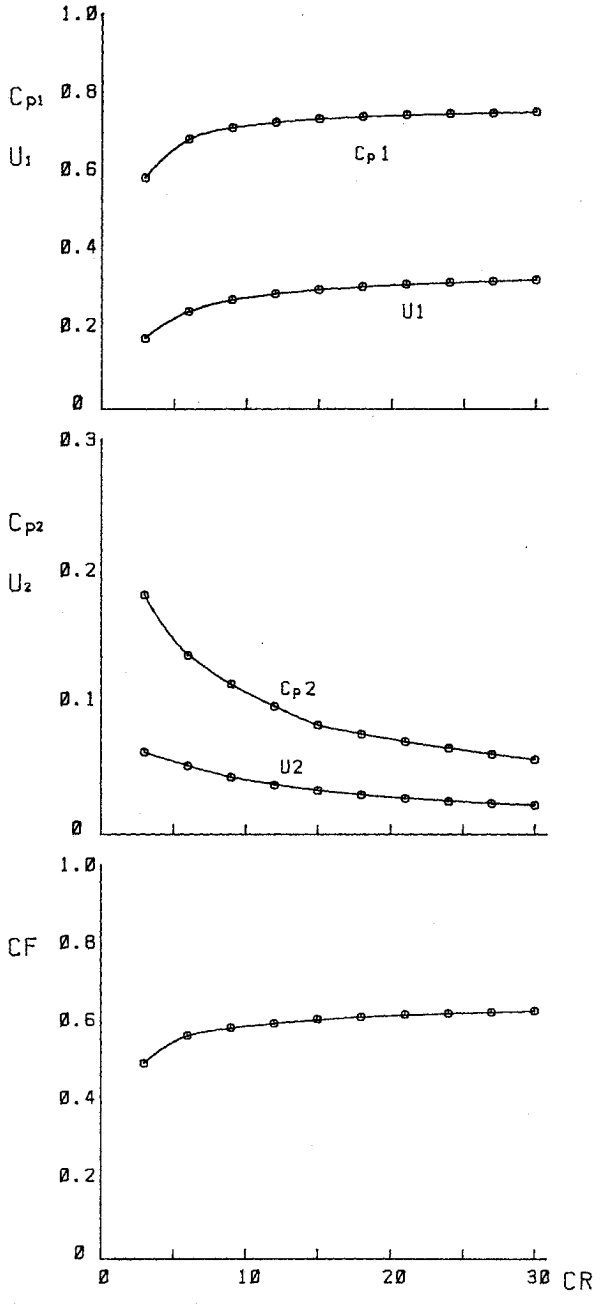

Fig. 5 Effect of contraction area ratio CR on the design criteria.

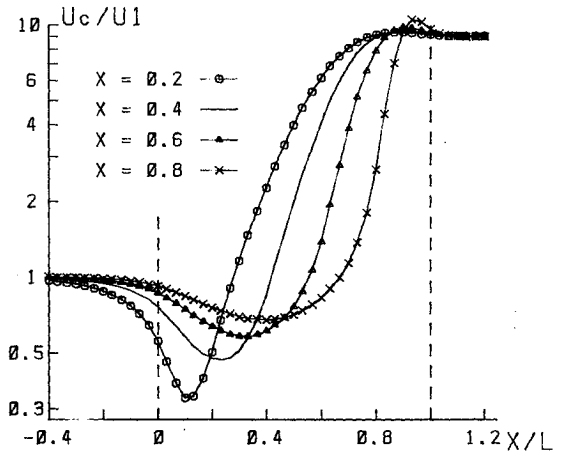

Fig. 4 Effect of X on velocity distributions at the corner.

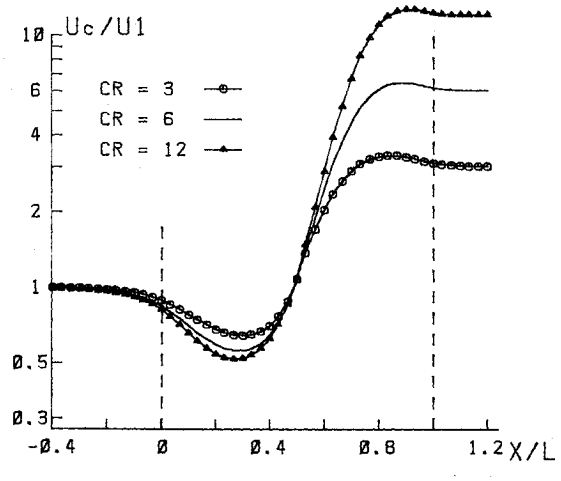

Fig. 6 Effect of CR on velocity distributions at the corner.

Table 1 Effect of CR on the choice of length L/D_1

Case	CR	X	Cp_1	Cp_2	$\bar{u}_2$	CF
1	9	0.50	0.7227	0.1158	0.0439	0.5954
2	12	0.53	0.7184	0.1041	0.0420	0.6053
3	12	0.56	0.7021	0.1095	0.0469	0.6042
4	12	0.50	0.7374	0.0987	0.0379	0.6075

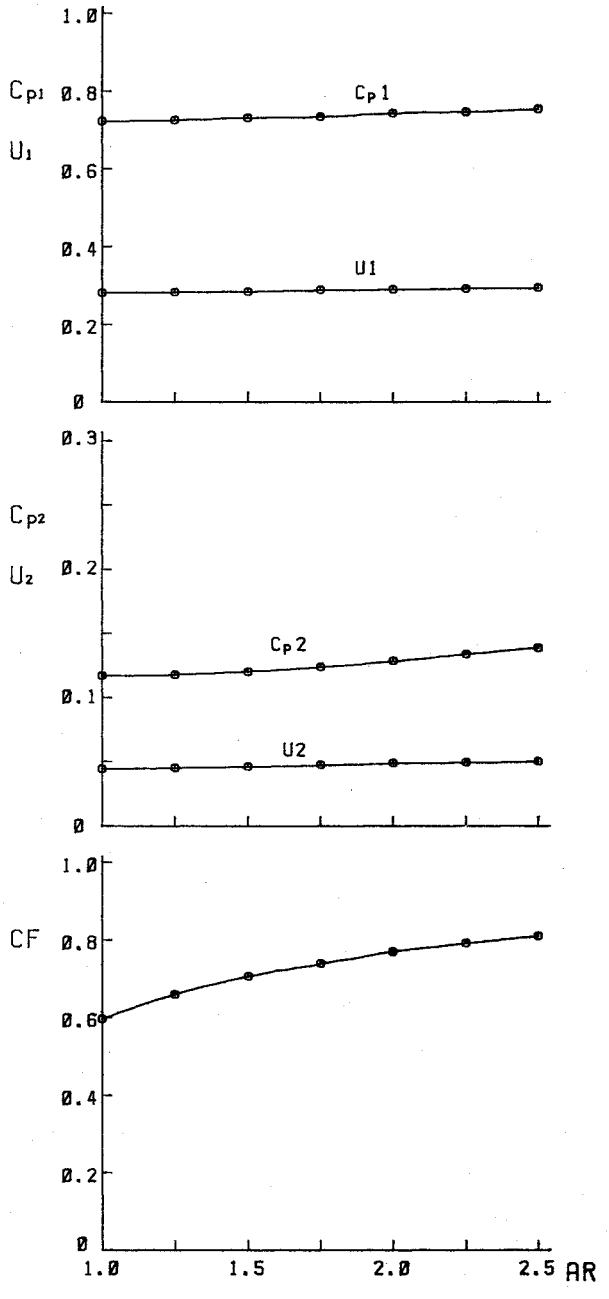

Fig. 7 Effect of section aspect ratio AR on the design criteria.

with increasing CR, it is found possible to reduce Cp_1 and Cp_2 simultaneously (see Table 1, case 1 vs case 2). That means that if Cp_1 and Cp_2 are held fixed, the required length L/D_1 can be reduced with increasing CR, a seemingly surprising result already pointed out by Morel for axisymmetric nozzles. However, if $\bar{u}_2$ is chosen as an exit criterion for comparison instead of Cp_2, this result may be changed (see Table 1, case 1 vs case 3). In any case, CR has only a weak influence on the length L/D_1. CR is also shown to affect the crossflow only weakly.

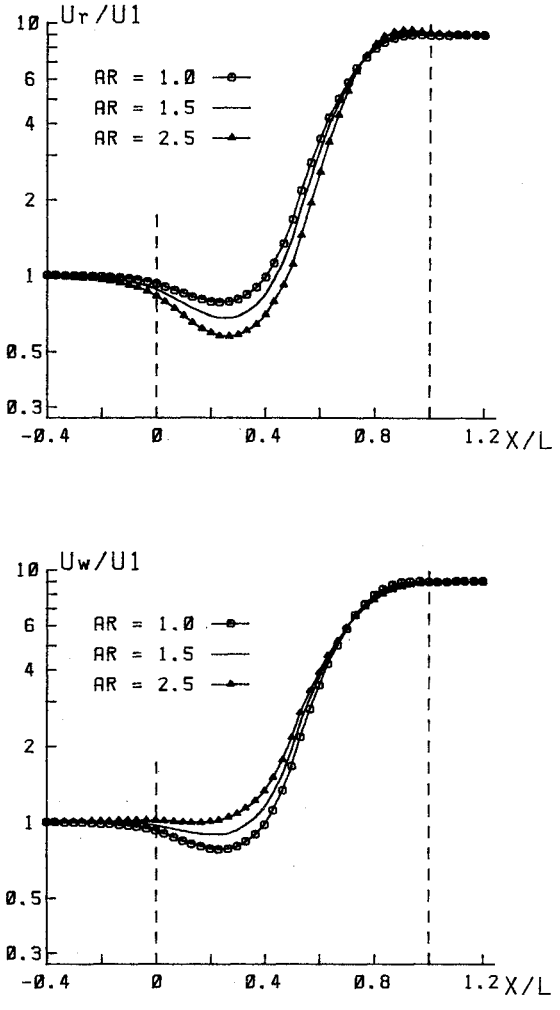

Fig. 8 Effect of AR on velocity distributions on the wall (Uw) and on the roof (Ur).

D. Aspect Ratio AR (for $AR1 = AR2$)

Here $AR1$ and $AR2$ are assumed equal and denoted with a single notation AR. In this study, flows in contractions with AR from 1 to 2.5 are calculated, ranging from a square cross section to a rather narrow one at both the exit and entrance. An examination of the computational results reveals that:

1) The increase of AR will enhance the pressure gradients and nonuniformities at the corner, but, rather unexpected, only to a very limited degree, as can be seen in Fig. 7.

2) As AR increases, the velocity extrema on the wall (wide side) will first decrease and then vanish completely, while on the roof (narrow side) they will increase gradually toward the value at the corner (see Fig. 8). This implies that the flow in the contraction will become more and more two-dimensional-like as AR increases. A sketch of isobars on the surface of the rectangular nozzle with $AR = 1$ and $AR = 2.5$ is presented in Fig. 9, illustrating the effect of AR on flow in the contraction.

3) The most important effect of AR is on the crossflow intensity. CF goes up evidently as AR increases (see Fig. 7).

E. Aspect Ratio $AR1 \neq AR2$

There exists the opinion that in designing three-dimensional contractions one should maintain cross section similarity so as to prevent the flow from "distortion." In the present study two groups of contractions with $AR1 \neq AR2$ were calculated. The first has $AR2 = 2.5$ with varying $AR1$, i.e., a fixed narrow test section (as in a two-dimensional wind tunnel) joined with settling chambers of various aspect ratio. It is

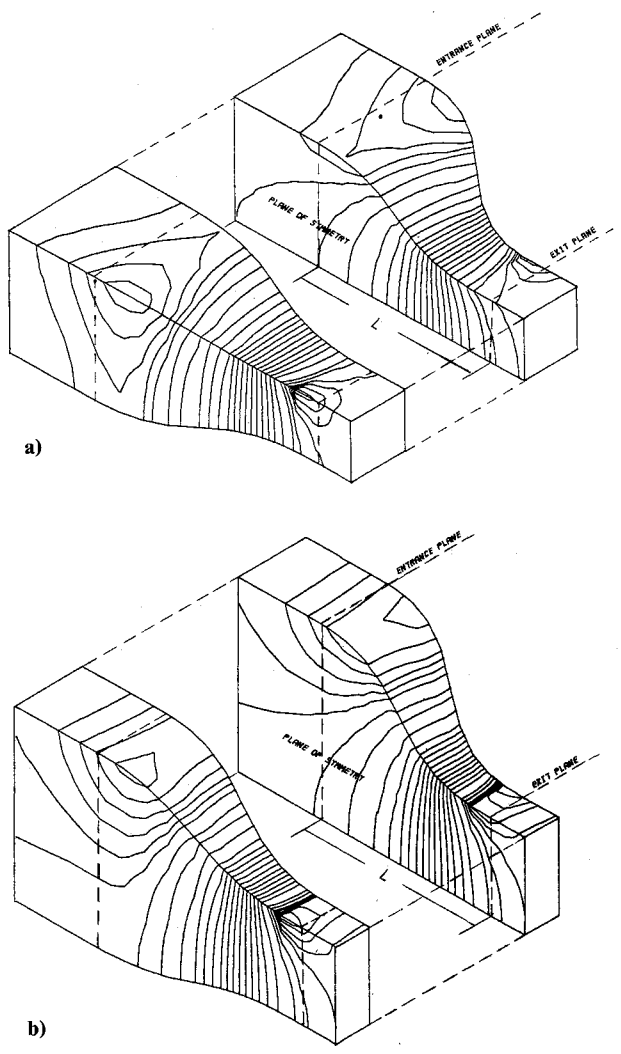

Fig. 9 Isobars on contraction surfaces. a) $AR = 1$; b) $AR = 2.5$.

interesting to find that flow conditions improve steadily as $AR1$ changes from 2.5 to 1. The case of $AR1 = 1$ (i.e., the poorest section similarity) gives the most favorable pressure gradients and flow uniformities, and good crossflow feature particularly (see Fig. 10).

The second group has contractions with $AR1 = 1$ and varying $AR2$, i.e., a fixed square settling chamber connected with test sections of various aspect ratio. The results are somewhat surprising. It is found that as $AR2$ increases, which means degrading both geometric symmetry and sectional similarity, the pressure gradients and nonuniformities are reduced slightly, rather than increased (see Fig. 11). Among them, the contraction with $AR1 = AR2 = 1$, i.e., square cross section with perfect geometric symmetry and similarity, turns out to have the worst values of Cp and $\bar{u}$, while the one with $AR1 = 1$ and $AR2 = 2.5$ gives the best of them. However, the situation is different if crossflow criteria are examined; the square contraction is still the best in this respect.

This investigation seems to suggest that contractions with cross section similarity actually have no special advantages. For narrow test sections this is perhaps the worst possible configuration. The results also suggest that a square cross section seems to be a good choice for the settling chamber no matter what the test section geometry may be.

F. Shape Parameter $Xw \neq Xr$

Here the effect of $Xw \neq Xr$ is examined. The results in Table 2 show that for $Xw/Xr = 0.5/0.3$ the values of Cp and $\bar{u}$ are something between those of 0.3/0.3 and 0.5/0.5, and the

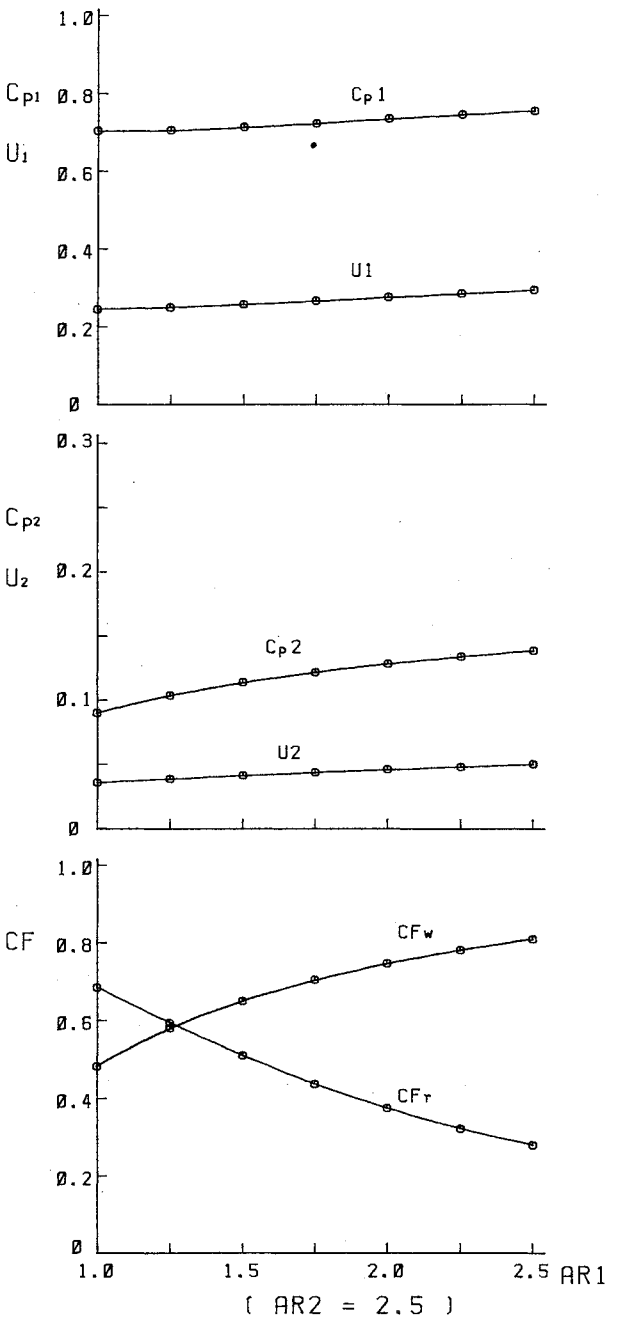

Fig. 10 Effect of varying $AR1$ ($AR2 = 2.5$).

criteria for 0.5/0.7 are between 0.5/0.5 and 0.7/0.7. This is all reasonable. It should be noted that the criteria mentioned above are all related to the corner. In fact, the influence of the Xw/Xr difference is mainly demonstrated in the augmentation of the velocity difference between the roof and the wall, usually leading to an increase of the crossflow criterion. Figure 12 shows the velocity distribution along the roof and the wall for different values of Xw/Xr. Evidently the roof/wall difference is augmented by the increase of the Xw/Xr difference.

There might be the possibility of achieving optimization by sophisticated compromise of different values for $AR1$, $AR2$, and Xw, Xr; however, in common practice it seems safer to choose the same value for Xr and Xw so as to avoid excessive crossflow.

G. Contour Power Factor n

Contraction contours of higher power are characterized by very smooth variations near the ends, whereas drastic area

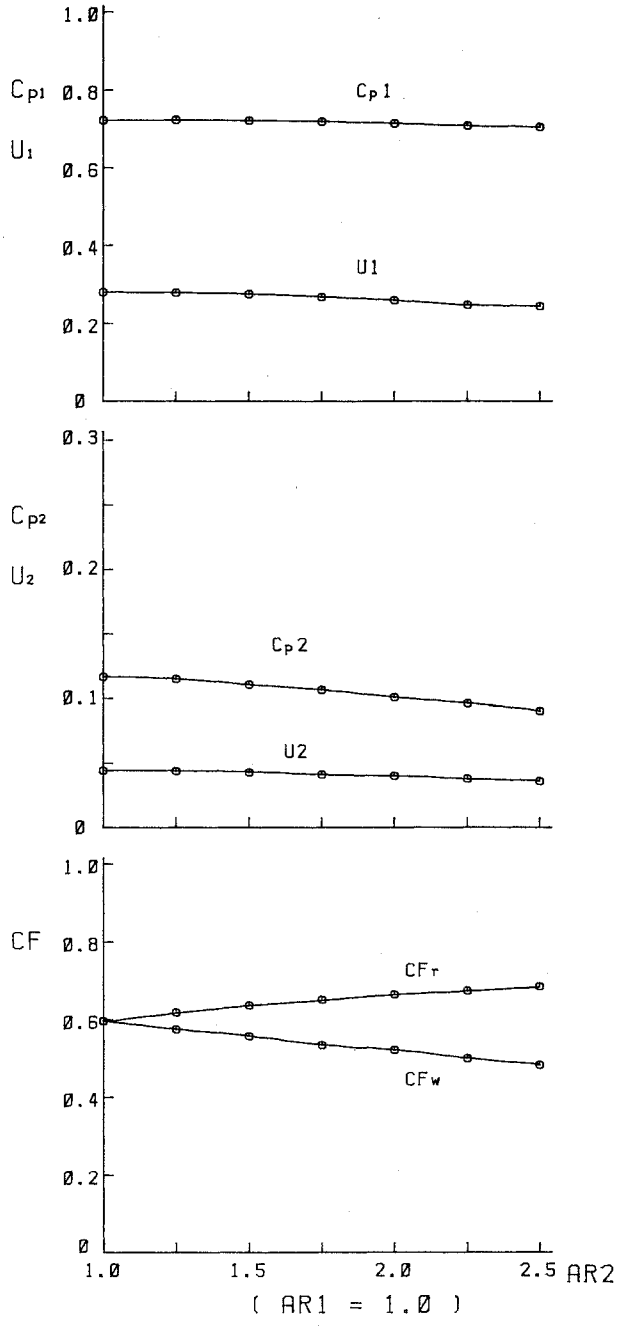

Fig. 11 Effect of varying *AR2* (*AR1* = 1.0).

variations occur inside the nozzle. To see the effect of these geometric features, contours for n from 4 to 9 are calculated and compared with a cubic contour. It is found that overshoot and undershoot are enhanced for contours of higher power, whereas the locations of their occurrence move inward (see Fig. 13). It is thought that these flow features are consistent with the geometry, namely the drastic contour variation inside the nozzle. Higher values of the Cp and a longer distance from the ends would have opposite effects on the flow uniformity. It turns out by computation that distance is the dominating factor. In all other figures above, an increase of Cp is always accompanied by an increase of nonuniformity $\bar{u}$, and vice versa. This situation is reversed in Fig. 14. In particular, the flow uniformity at the exit is improved significantly for higher power contours. This is shown strikingly in the $\bar{u}_2$ plot of Fig. 14. The crossflow property is found to become poorer as power factor n is increased.

Table 2 Effect of *Xw*/*Xr* difference

Case	*Xw*	*Xr*	Cp_1	Cp_2	$\bar{u}_2$	*CF*
1	0.3	0.3	0.8389	0.0668	0.0192	0.6967
2	0.5	0.5	0.7227	0.1158	0.0439	0.5958
3	0.7	0.7	0.6028	0.1835	0.0961	0.5811
4	0.5	0.3	0.7748	0.0972	0.0344	0.7329
5	0.5	0.7	0.6624	0.1488	0.0710	0.7300

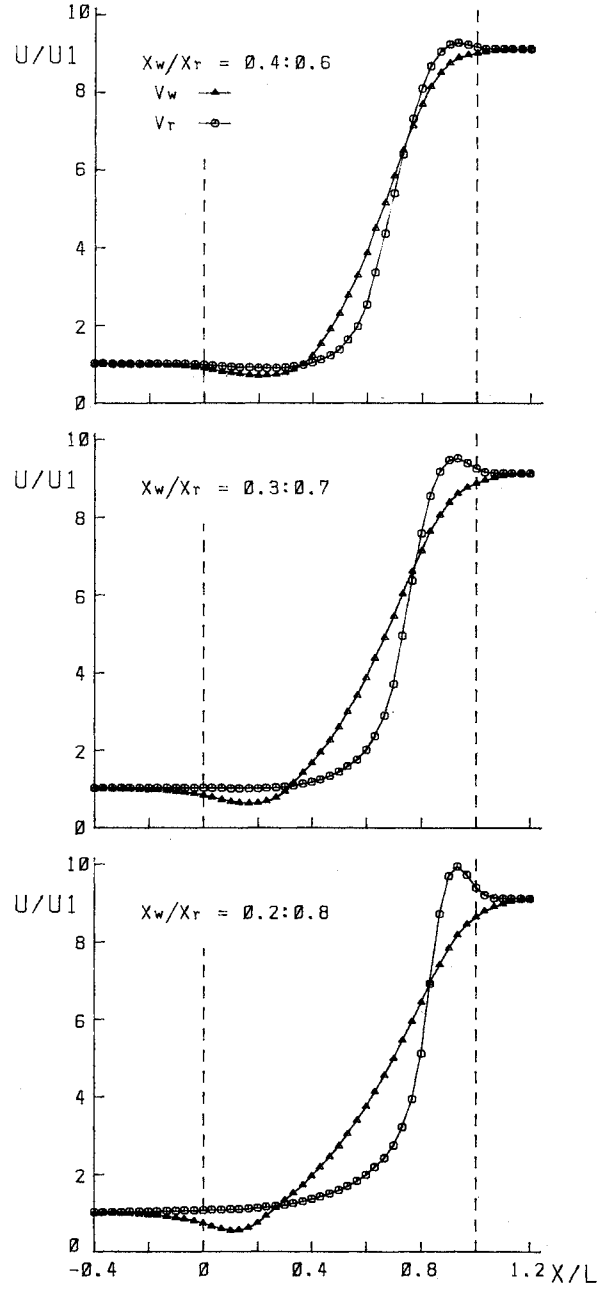

Fig. 12 Different velocity distributions along the roof and the wall for contractions of *Xw* ≠ *Xr*.

In contraction design, the criteria of most importance are Cp_1 and $\bar{u}_2$. The above discussion indicates that contours of higher power are beneficial for the aft part of the nozzle but unfavorable for the fore section. It seems advantageous to have contraction contours matched with a cubic fore part and a higher power aft part (e.g., $n = 7$). Computation of flow in such a contraction was conducted. It is shown (see Table 3) that the contraction has much better exit uniformity, while Cp_1 and $\bar{u}_1$ and crossflow criteria are nearly unchanged compared to those of the cubic contour.

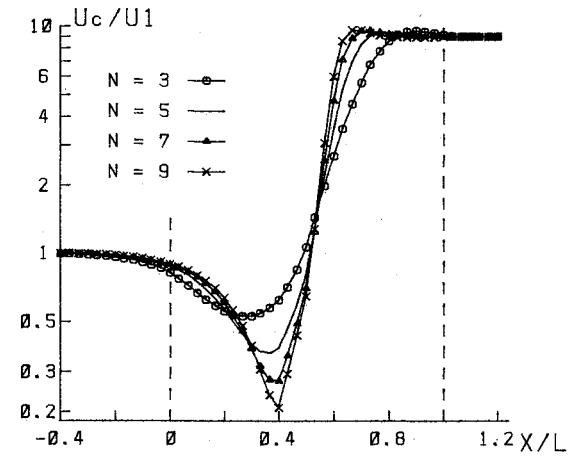

Fig. 13 Effect of contour power factor n on velocity distributions at the corner.

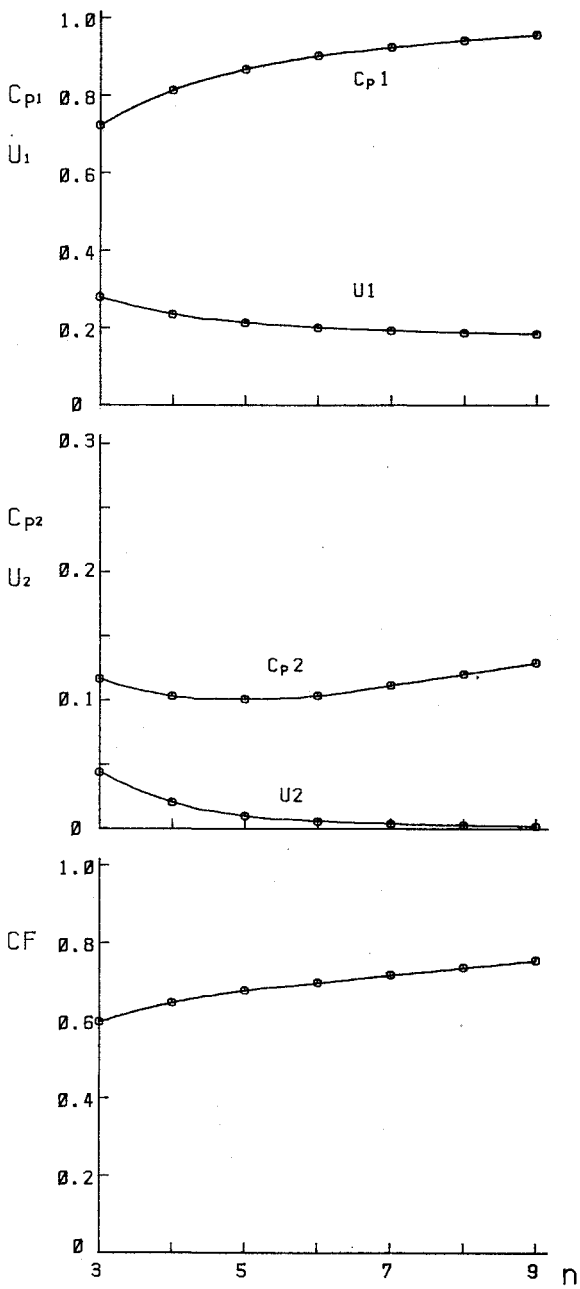

Fig. 14 Effect of n on the design criteria.

Table 3 Comparison of different contraction contours

Case	n	Cp_1	Cp_2	$\bar{u}_2$	CF
1	3	0.7227	0.1158	0.0439	0.5958
2	7	0.9251	0.1129	0.0035	0.7175
3	3/7	0.7282	0.1414	0.0107	0.6162

V. Conclusions

A numerical analysis of incompressible potential flow in rectangular contractions has been conducted. Criteria for the design of the contractions have been suggested and discussed. Comparative parametric studies have been carried out in which the influences of various parameters are examined. The results indicate the following:

1) The effects of CR, L/D_1, and X on criteria Cp and sectional nonuniformity $\bar{u}$ are similar qualitatively, but stronger quantitatively due to the corner effect, compared to those of axisymmetric contractions. Increasing L/D_1 improves the crossflow condition effectively, while CR and X have only limited influences on the crossflow.

2) An increase of cross section aspect ratio AR will reduce the velocity extrema on the wall axis (the wide side) and increase those on the roof axis, whereas the velocity extrema at the corner are only increased slightly. The flow in the contraction will become more two-dimensional-like, and the crossflow intensity (on the wall) will increase significantly.

3) There seems to be no advantage of designing contractions with cross section similarity. This is perhaps the worst possible geometry for two-dimensional wind tunnels with narrow test sections. Square cross section seems to be a good choice for settling chambers no matter what the test section geometry may be.

4) Different values of Xw and Xr are not recommended because the velocity differences between the wall and the roof will be augmented, and stronger crossflow may result.

5) Contours of higher power n will improve the flow uniformity $\bar{u}$ at the end sections, in spite of causing stronger pressure gradients. This is good for the aft part of the nozzle but unfavorable for the fore. A family of contours with cubic fore parts matched with higher power aft parts is suggested. The contours are shown to perform favorably both at the entrance and at the exit.

References

[1]Cheers, F., "Notes on Wind Tunnel Contractions," ARC R&M 2137, 1945.

[2]Whitehead, L. G., Wu, L. Y., and Waters, M. H. L., "Contracting Ducts of Finite Length," *Aeronautical Quarterly*, Vol. II, 1951, pp. 254–271.

[3]Libby, P. A., and Reiss, H. R., "The Design of Two-Dimensional Contraction Sections," *Quarterly of Applied Mathematics*, Vol. IX, 1951, pp. 95–98.

[4]Tsien, H., "On the Design of the Contraction Cone for a Wind Tunnel," *Journal of the Aeronautical Sciences*, Vol. 10, Feb. 1943, pp. 68–70.

[5]Szczeniowski, B., "Contraction Cone for a Wind Tunnel," *Journal of the Aeronautical Sciences*, Vol. 10, Oct. 1943, pp. 311–312.

[6]Smith, R. H., and Wang, C. T., "Contraction Cones Giving Uniform Throat Speeds," *Journal of the Aeronautical Sciences*, Vol. 11, 1944, pp. 356–360.

[7]Thwaites, B., "On the Design of Contractions for Wind Tunnels," ARC R&M 2278, 1946.

[8]Cohen, M. J., and Ritchie, N. J. B., "Low-Speed Three-Dimensional Contraction Design," *Journal of Royal Aeronautical Society*, Vol. 66, 1962, pp. 231–236.

[9]Jordinson, R., "Design of Wind-Tunnel Contractions," *Aircraft Engineering*, Vol. 33, 1961, pp. 294–297.

[10]Barger, R. L., and Bowen, J. T., "A Generalized Theory for the Design of Contraction Cones and Other Low-Speed Ducts," NASA TN D-6962, 1972.

[11]Morel, T., "Comprehensive Design of Axisymmetric Wind Tunnel Contractions," *Journal of Fluids Engineering, ASME Transactions*, Series I, Vol. 97, June 1975, pp. 225–233.

[12]Morel, T., "Design of Two-Dimensional Wind Tunnel Contractions," *Journal of Fluids Engineering, ASME Transactions*, Series I, Vol. 99, June 1977, pp. 371–378.

[13]Chmielewski, G. E., "Boundary Layer Considerations in the Design of Aerodynamic Contractions," *Journal of Aircraft*, Vol. 11, Aug. 1974, pp. 435–438.

[14]Borger, G. G., "The Optimization of Wind Tunnel Contractions for the Subsonic Range," NASA TTF-16899, March 1976.

[15]Mikhail, M. N., "Optimum Design of Wind Tunnel Contractions," *AIAA Journal*, Vol. 17, No. 5, 1979, pp. 471–477.

[16]Sanderse, A., and van der Voreen, J., "Finite Difference Calculations of Incompressible Flows Through a Straight Channel of Varying Rectangular Cross-Section," NLR TR 77109U, Sept. 1977.

[17]Downie, J. H., Jordinson, R., and Barnes, F. H., "On the Design of Three-Dimensional Wind Tunnel Contractions," *Aeronautical Journal*, Vol. 88, Aug./Sept. 1984, pp. 287–295.

[18]Batill, S. M., and Hoffman, J. J., "The Aerodynamic Design of Three-Dimensional, Subsonic Wind Tunnel Inlets," *AIAA Journal*, Vol. 24, No. 2, 1986, pp. 268–269.